

# Biomechanics of the knee joint in flexion under various quadriceps forces

W. Mesfar, A. Shirazi-Adl\*

*Génie mécanique, École Polytechnique, Montréal, Québec, Canada*

Received 3 January 2005; received in revised form 7 March 2005; accepted 22 March 2005

## Abstract

Bioemchanics of the entire knee joint including tibiofemoral and patellofemoral joints were investigated at different flexion angles ( $0^\circ$  to  $90^\circ$ ) and quadriceps forces (3, 137, and 411 N). In particular, the effect of changes in location and magnitude of restraining force that counterbalances the isometric extensor moment on predictions was investigated. The model consisted of three bony structures and their articular cartilage layers, menisci, principal ligaments, patellar tendon, and quadriceps muscle. Quadriceps forces significantly increased the anterior cruciate ligament, patellar tendon, and contact forces/areas as well as the joint resistant moment. Joint flexion, however, substantially diminished them all with the exception of the patellofemoral contact force/area that markedly increased in flexion. When resisting extensor moment by a force applied on the tibia, the force in cruciate ligaments and tibial translation significantly altered as a function of magnitude and location of the restraining force. Quadriceps activation generated large ACL forces at full extension suggesting that post ACL reconstruction exercises should avoid large quadriceps exertions at near full extension angles. In isometric extension exercises against a force on the tibia, larger restraining force and its more proximal location to the joint substantially decreased forces in the anterior cruciate ligament at small flexion angles whereas they significantly increased forces in the posterior cruciate ligament at larger flexion angles.

© 2005 Elsevier B.V. All rights reserved.

**Keywords:** Knee joint; Flexion angle; Quadriceps load; Finite element analysis; Kinematics; Ligament forces; Contact forces; Boundary conditions

## 1. Introduction

In various recreational and sport activities, both patellofemoral and tibiofemoral joints undergo large forces (exceeding body weight) and moments while accommodating the considerable knee joint mobility. The primary function of the patella is to increase the effective lever arm of quadriceps muscle forces required to resist or generate extensor moments. In doing so, the patellofemoral joint is frequently the source of the knee anterior pain related to disturbances in normal tracking, instability, and excessive pressure syndrome. Patellofemoral pain is a principal health problem accounting for 33.2% of all knee disorders in women and 18.1% of those in men [1]. Excessive contact pressure can be a cause of patellofemoral pain

leading to degeneration of the articular cartilage. Bio-mechanical investigation of the entire knee joint is essential in understanding the joint function and interactions between various components in both intact and perturbed conditions. An improved knowledge can be of great help not only in prevention and rehabilitation procedures but also in the design of better reconstruction and implant systems in the management of knee joint disorders.

Measurement studies have demonstrated the interactions between the extensor mechanism and the entire knee joint mechanics. Many have investigated the joint kinematics [2–8], ligament forces/strains [9–14], or contact forces/areas [8,16–23]. The extensor mechanism or quadriceps muscle group has often been represented by a single muscle (rectus femoris, RF) [17,21,23–29]. This risks to influence the patellofemoral kinematics and contact pressure [7,16,30] which stresses the importance in accurate representation of extensor mechanism. To counterbalance the extensor moment of quadriceps forces

\* Corresponding author. Department of Mechanical Engineering, Ecole Polytechnique, P.O. 6079, Station 'centre-ville', Montreal, Quebec, Canada H3C 3A7. Tel.: +1 514 3404711x4129.

E-mail address: [abshir@meca.polymtl.ca](mailto:abshir@meca.polymtl.ca) (A. Shirazi-Adl).

at different flexion angles, measurement studies also often apply a restraining force on the tibia at various positions away from the joint [12–14,16,31–36]. This restraint causes a posterior shear force on the tibia that influences, depending on the joint flexion and quadriceps forces, the magnitude of ACL force and tibial anterior translation [34,35].

In contrast to measurements, attempts to simulate the tibiofemoral or patellofemoral joints by finite element model studies have been scarce. To obtain accurate results, model studies should account, amongst others, for the realistic 3-D geometry especially of the articular surfaces, compliant cartilage layers, menisci, ligaments (with non-linear properties and initial strains), quadriceps muscle components, and proper boundary/loading conditions. Due to the complexity of the entire knee joint, previous works have considered either the patellofemoral joint [26] or the tibiofemoral joint [37–43] and not both together. For the patellofemoral joint, Heegaard et al. [26] developed a 3-D finite element model to study its response under 40 N applied via the RF component at joint flexion angles of 30° to 135°. The patella was deformable but the femur was rigid without cartilage layer.

In this study and as a continuation of our earlier works on the tibiofemoral joint [37,38,41–43], we aimed to develop a novel 3-D finite element model of the entire knee joint incorporating both the tibiofemoral and patellofemoral joints, a complex model that has not yet been reported. Apart from the investigation of the joint mechanics in flexion (0°–90°) under various quadriceps forces, this study aimed to examine the influence of the tibial constraint under quadriceps forces. It is hypothesized

that the manner in which the tibia is restrained could influence the results. Simulation of various pathologic conditions (e.g., ligament deficiency) will be performed in future studies.

## 2. Method

The finite element model of the knee joint consists of three bony structures (tibia, femur, and patella) and their articular cartilage layers, menisci, six principal ligaments (collaterals LCL/MCL, cruciates ACL/PCL, and medial/lateral patellofemoral ligaments MPFL/LPFL), patellar tendon PT, and quadriceps muscle vectors (divided into three components VL/RF-VIM/VMO) (Fig. 1). Bony structures (i.e., femur, tibia and patella) are represented by rigid bodies due to their much greater stiffness as compared with joint soft tissues. Menisci are modelled as non-homogeneous composites of a bulk material reinforced by radial and circumferential collagen fibres. Ligaments are each modeled by a number of uniaxial elements with different prestrain (or pretension) values and nonlinear material properties (no compression) based on those used in our earlier model studies and/or reported in the literature (Fig. 2) [41,42,44–46]. The medial patellofemoral ligament (MPFL) is represented by four elements, the lateral patellofemoral ligament (LPFL) by three, and the patellar tendon (PT) by nine (Fig. 1). The articular cartilage layers over tibia, femur, and patella are considered homogeneous isotropic with elastic modulus of 12 MPa and Poisson's ratio of 0.45. The matrix of menisci (apart from the reinforcing nonlinear collagen fibres) is also assumed isotropic with 10

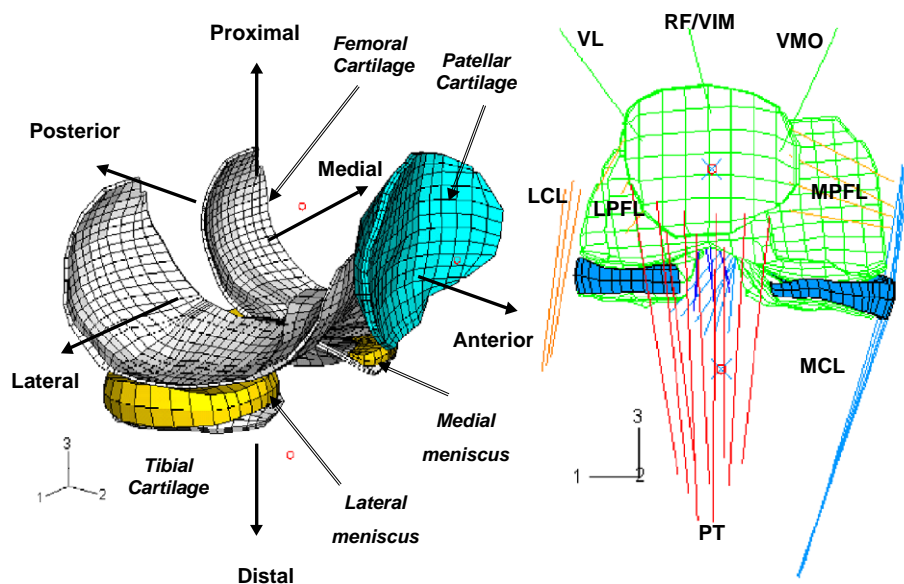


Fig. 1. The knee joint finite element models showing cartilage layers, menisci, ligaments, patellar tendon, and quadriceps muscles. Bony structures are shown only by their primary nodes. Quadriceps components considered are VMO: vastus medialis obliquus, RF: rectus femoris, VIM: vastus intermedius medialis, and VL: vastus lateralis (VL). LPFL: lateral patellofemoral ligament, MPFL: medial patellofemoral ligament.

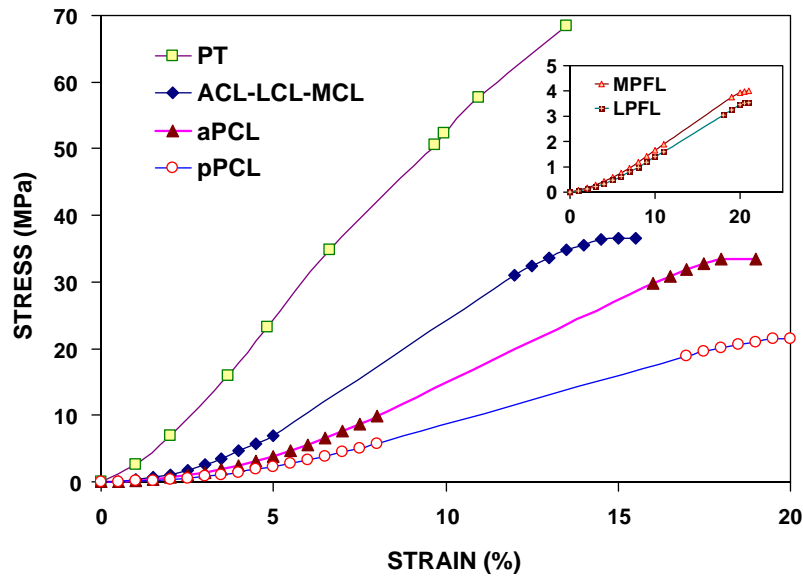


Fig. 2. Stress–strain curves for various ligaments used in the model and the patellar tendon, PT. ACL: anterior cruciate ligament, LCL: lateral collateral ligament, MCL: medial collateral ligament, aPCL/pPCL: anterior/posterior bundles of posterior cruciate ligament, MPFL/LPFL: medial/lateral patellofemoral ligaments.

MPa for the elastic modulus and 0.45 for the Poisson's ratio. Each meniscus matrix is stiffened by a higher modulus of 15 MPa at both ends ( $\sim 5$  mm length) where inserted into the tibia to simulate its horns. Articulations at the cartilage–cartilage (in tibiofemoral and patellofemoral joints) and cartilage–meniscus (in tibiofemoral joint at both meniscal distal and proximal surfaces) are simulated using a large displacement frictionless hard contact algorithm with no penetration allowed. Total ligament initial cross-sectional areas are taken as 42, 60, 18, 25, 99, 42.7, and 28.5 mm<sup>2</sup> for the ACL, PCL, LCL, MCL, PT, MPFL, and LPFL, respectively.

To simulate a stable and fully unconstrained flexion response, the femur is fixed while the tibia and the patella are left completely free. The joint reference configuration at full extension is initially established under ligament prestrains and quadriceps forces. The quadriceps muscle components are each simulated by an element [16] with predefined load-displacement relationships with constant force at all displacements. To evaluate the influence of changes in the quadriceps force magnitude on the response, three values of 3 N (i.e., passive motion), 137 N and 411 N are considered. The quadriceps load of 137 N, for example, accounts for 40 N in vastus medialis obliquus (VMO), 60 N in rectus femoris/vastus intermidus medialis (RF/VIM), and 50 N in vastus lateralis (VL). This magnitudes are selected according to the ratios of their physiological cross-sectional areas VMO:RF/VIM:VL = 2:3:2.5 [7]. The direction of the force in each component is derived from the  $Q$ -angle model ( $Q$  angle = 14°) [7]. In the frontal plane, the direction of RF/VIM is parallel to the femoral axis, the VMO is 41° medially, and the VL 22° laterally. In the sagittal plane, RF/VIM is 4° anterior to the femoral axis whereas the VMO and VL are oriented

parallel to the femoral axis. Following the application of prestrains in ligaments and forces in quadriceps yielding the reference kinematics configuration for subsequent analyses, the tibia is subjected to incremental flexion rotation varying from 0° to 90° under constant quadriceps preloads.

Due to the presence of finite rotations at the tibia and patella, the 3-D motion of these bodies is characterised by a proper joint coordinate system [47]. The tibial varus–valgus and internal–external rotations as well as patellar medial–lateral rotation and tilt are defined about their respective bony local convective coordinates systems. The configuration of patella and tibia at each instant of loading is hence defined by three translations along global axes and three Euler angles. The non-linear elastostatic analysis is performed using ABAQUS (version 6.3) finite element package program. To evaluate the finite element mesh and its likely influence on predictions, a convergence study is initially carried out with three levels of mesh refinement under 137 N quadriceps force. The total number of 8-node solid elements at articular surfaces varied in these studies from 879 to 1222 and further to 2440.

To evaluate the impact of the reversal of boundary conditions on predictions, another condition is also considered in which the femur is subjected to flexion. The femoral translations (medial–lateral, posterior–anterior and distal–proximal) are left free along with the tibial coupled rotations (varus–valgus and internal–external). After establishing the reference configuration under ligament prestrains and quadriceps force (137 N), the femur is incrementally flexed from 0° to 90°. Moreover, to investigate the effect of tibial constraint on results, additional cases are studied in which the constraint is provided by a

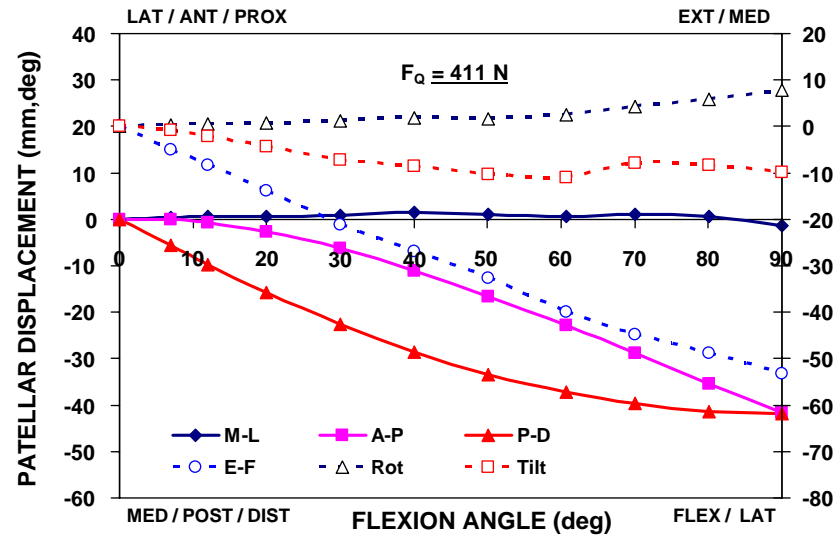


Fig. 3. Patellar displacements (translations on the left axis and rotations on the right) under quadriceps loading of 411 N at different flexion angles. The translations are in the global anatomical directions: medial–lateral (M–L), anterior–posterior (A–P), and proximal–distal (P–D). The rotations are the extension–flexion (Ext–flex), medial–lateral rotation and medial–lateral tilt defined as Euler angles. The results for  $F_Q=3$  and 137 N are not shown to avoid confusion.

perpendicular force rather than a pure sagittal moment. Under 411 N quadriceps and at 0° and 90° joint angles, the tibia is subjected to perpendicular restraining forces with varying magnitudes at 20 or 30 cm distal to the tibiofemoral joint level.

### 3. Results

The convergence study demonstrated a negligible change in predictions on kinematics and load distribution as the mesh was refined. For example at 60° flexion under  $F_Q=137$  N, the patellar tendon force changed from 78.9

to 80.8 N and to 77.8 N whereas the total patellofemoral contact force varied from 118.3 to 118.2 N and to 118.1 N as the mesh was refined. At 0° flexion, ACL force varied from 85.0 to 84.1 N and to 89.4 N, patellofemoral contact force from 65.2 to 65.0 N and to 64.9 N, and patellar tendon force from 130.4 to 127.9 N and to 131.7 N as the mesh was refined, respectively. Differences in computed kinematics were even smaller.

#### 3.1. Joint kinematics

Results are presented with respect to the reference configuration following application of either ligament pre-

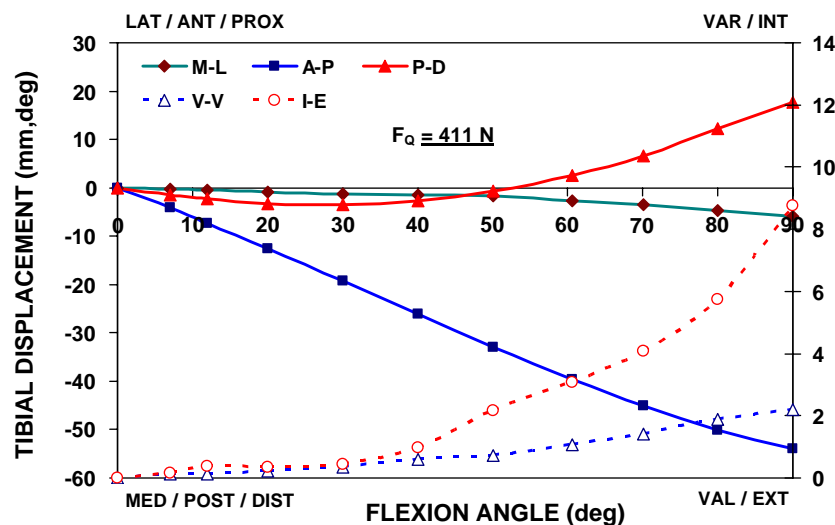


Fig. 4. Tibial displacements (translations on the left axis and rotations on the right) under quadriceps loadings of 411 N at different flexion angles. The three global tibial translations are: anterior–posterior (A–P), medial–lateral (M–L), and proximal–distal (P–D) whereas the tibial rotations are: varus–valgus (V–V) and internal–external (I–E) rotations with respect to local system as Euler angles. The results for  $F_Q=3$  and 137 N are not shown to avoid confusion.

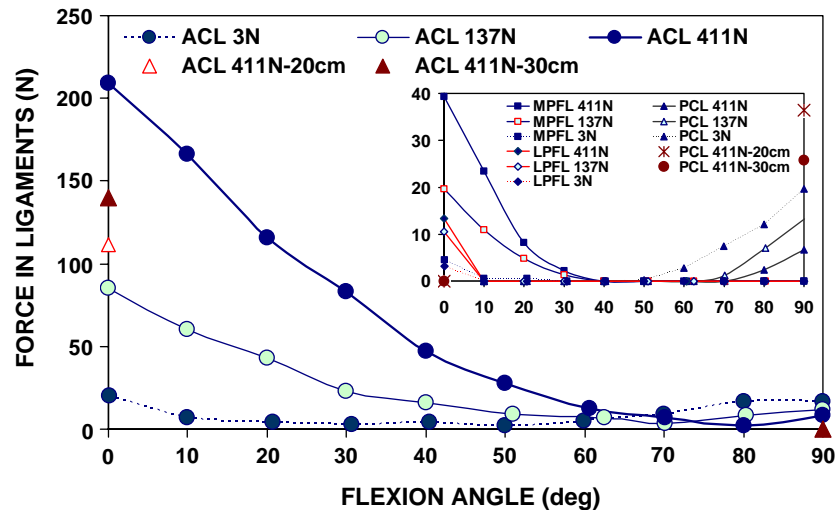


Fig. 5. Computed forces in the anterior/posterior cruciate and medial/lateral patellofemoral ligaments at different flexion angles under  $F_Q=3, 137$ , and  $411$  N. Cruciate ligament forces at  $0^\circ$  and  $90^\circ$  are also shown for the cases in which the extensor moment is resisted by a restraining force located either at 20 or 30 cm distal to the joint.

strains alone for the data at full extension or ligament prestrains with quadriceps forces for the data in flexion. At full extension, the patella shifted laterally by  $\sim 0.2, 3$ , and  $4$  mm, displaced proximally by  $\sim 0, 2.8$ , and  $4.2$  mm, and flexed by  $\sim -3^\circ, 3.1^\circ$ , and  $4^\circ$ , under quadriceps forces of  $3, 137$ , and  $411$  N, respectively. Under quadriceps forces and in flexion, the patella translated posteriorly and distally while rotating medially and tilting laterally (Fig. 3).

At full extension, the tibia displaced anteriorly by  $\sim -0.6, 1.9$ , and  $3.7$  mm, proximally by  $\sim -0.15, 0.5$ , and  $0.8$  mm, rotated externally by  $\sim -2^\circ, 3^\circ$ , and  $7^\circ$ , and rotated in varus direction by  $\sim -0.2^\circ, 0.6^\circ$ , and  $1.1^\circ$  as the quadriceps loading increased from  $3$  to  $137$  N and further to  $411$  N, respectively. During the knee flexion, the tibia moved in medial, posterior and proximal

directions while rotating in internal and varus directions (Fig. 4).

### 3.2. Load distribution

At full extension, large forces were generated in the ACL while almost the entire applied quadriceps forces were supported by the patellar tendon, PT (Figs. 5 and 6). Both PT and ACL forces, however, substantially diminished with the joint flexion. In contrast, the PCL mechanical role initiated at larger flexion angles reaching, at  $90^\circ$  flexion,  $\sim 20, 13$ , and  $7$  N under  $3, 137$ , and  $411$  N quadriceps forces, respectively (Fig. 5). For all quadriceps forces, the patellofemoral ligaments, MPFL and LPFL, supported small loads at full extension that disappeared as the joint flexed

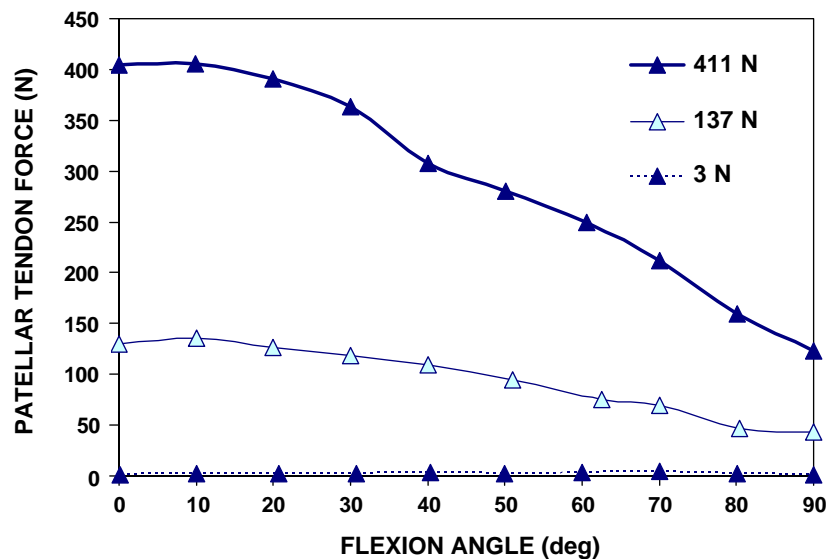


Fig. 6. Computed forces in the patellar tendon at different flexion angles under  $F_Q=3, 137$ , and  $411$  N. No noticeable changes are computed when the extensor moment is resisted by a restraining force at 20 or 30 cm distal to the joint (not shown).

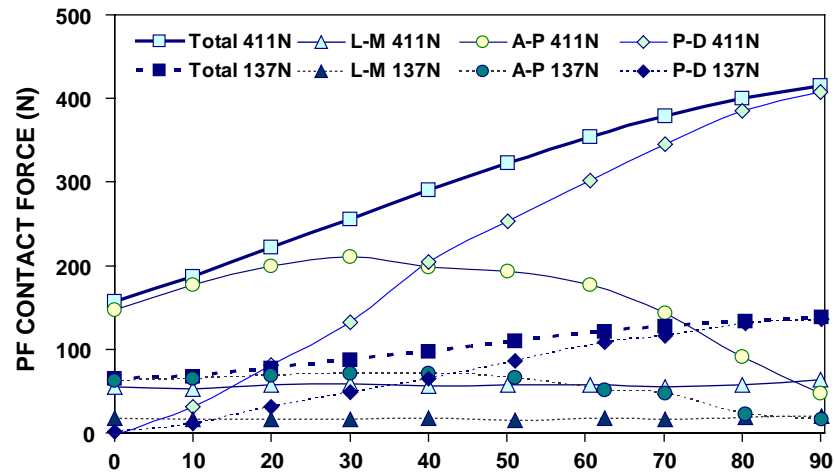


Fig. 7. Total resultant patellofemoral contact force and its components in different anatomical directions as a function of joint flexion under  $F_Q=137$  and 411 N. No noticeable changes are computed when the extensor moment is resisted by a restraining force at 20 or 30 cm distal to the joint (not shown).

(Fig. 5). Forces in MCL and LCL remained nearly small  $<40$  N at all joint flexion angles and quadriceps forces considered, the latter increased slightly in flexion whereas the former decreased slightly in flexion and with smaller quadriceps forces.

The total PF contact force (Fig. 7) and contact area (Fig. 9) increased with both knee flexion and quadriceps forces. The contact force orientation changed with flexion being primarily in anterior–posterior direction at smaller flexion angles and in axial direction at larger flexion angles (Fig. 7). The total TF contact force (Fig. 8) and contact area (Fig. 9) increased with quadriceps forces but decreased with flexion angle. For the passive case ( $F_Q=3$  N), in contrast, the contact force and area increased with knee flexion; i.e., contact force increased from 62 N at full

extension to 98 N at  $90^\circ$  of flexion. The tibiofemoral contact force changed orientation from axial direction at full extension to anterior–posterior at  $90^\circ$  flexion (Fig. 8). The lateral compartment at the TF contact carried, at all flexion angles, a larger proportion of the total load than did the medial compartment.

The joint resistant extensor moment significantly increased with greater  $F_Q$  but decreased with flexion angle (Fig. 10). The passive joint offered a small resistance remaining  $<0.4$  N-m throughout flexion.

### 3.3. Boundary conditions

For the second set of boundary conditions with the femur, rather than the tibia, undergoing flexion and under

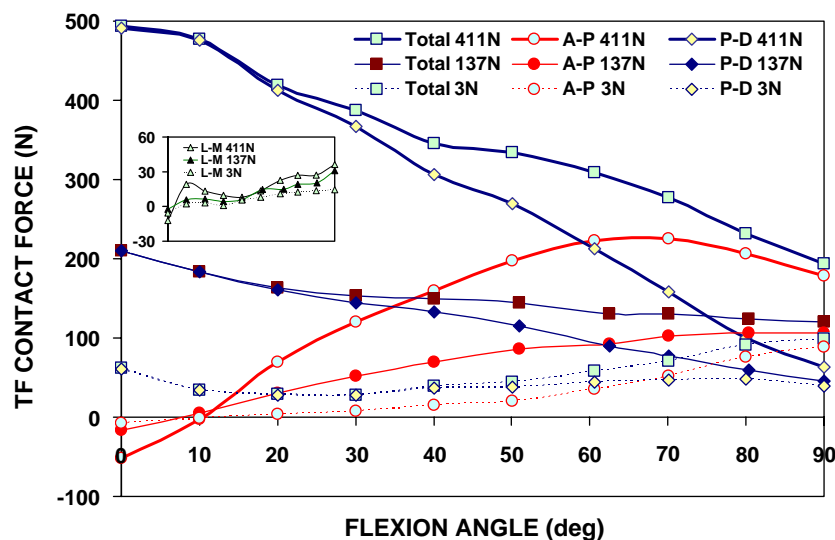


Fig. 8. Total resultant tibiofemoral contact force and its components in different anatomical directions as a function of joint flexion under  $F_Q=3$ , 137 and 411 N. The lateral–medial component is  $<40$  N and shown separately. No noticeable changes are computed when the extensor moment is resisted by a restraining force at 20 or 30 cm distal to the joint (not shown).



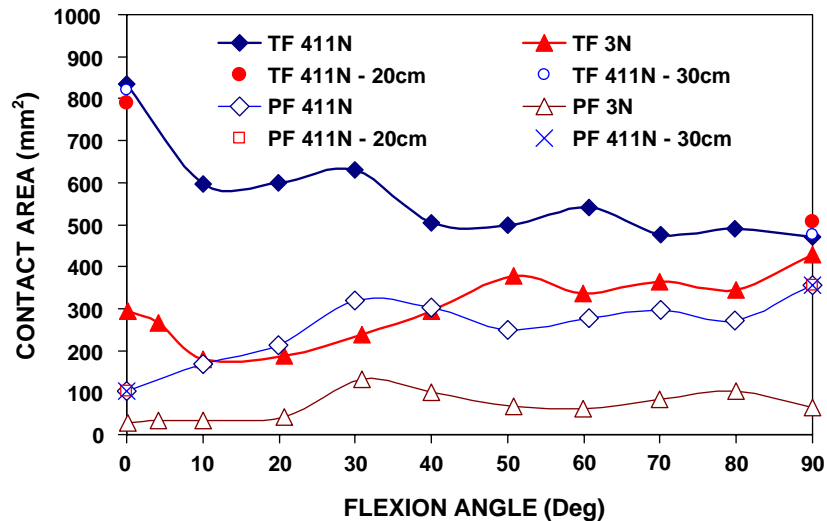


Fig. 9. Total tibiofemoral and patellofemoral contact areas under  $F_Q=3$  and 411 N at different flexion angles. Small changes are computed at 0° and 90° when the extensor moment is resisted by a restraining force at 20 and 30 cm distal to the joint.

$F_Q=137$  N, the patella translates posteriorly (1.6 mm at 0° and 28.1 mm at 90°), shifts laterally (2.2 mm at 0° and 7.0 mm at 90°), tilts laterally (3.3° medially at 0° and 9.5° laterally at 90°), flexes medially (−4° at 0° and 35° at 90°), and rotates medially (4.5° at 0° and 11.2° at 90°). The patellar tilt and medial rotation remain similar to those in Fig. 3. The femur translates laterally, posteriorly, and proximally while the tibia rotates in internal and varus directions. The PT and ligament forces remain unchanged. The total PF and TF contact forces (but not their relative components) and contact areas remain similar to those predicted for the reference boundary case.

Restraining the tibia by perpendicular forces located at 20 or 30 cm from the joint level rather than by pure sagittal moments, influences primarily the tibial translation in the direction of applied force resulting in increases of 1 or 0.7 mm at full extension and of 2 or 1.5 mm at 90°, respectively.

The required restraining forces are calculated to reach 82.5 and 23 N at 0° and 90°, respectively, when located at 20 cm which decrease to 56.1 and 15.7 N at 30 cm. These forces significantly diminish ACL force (Fig. 5) by ~50% at full extension. In contrast, they substantially increase PCL force at 90° from 6.7 to 25.7 N and 36.4 N, respectively (Fig. 5). Forces in the LCL increase whereas those in the MCL slightly decrease in presence of restraining forces. The TF contact force slightly alters (by <22 N) whereas the PF contact force remains nearly the same (by <3 N) in these cases.

#### 4. Discussion

In this study, based on a validated tibiofemoral model, a realistic 3-D non-linear model of the knee joint including

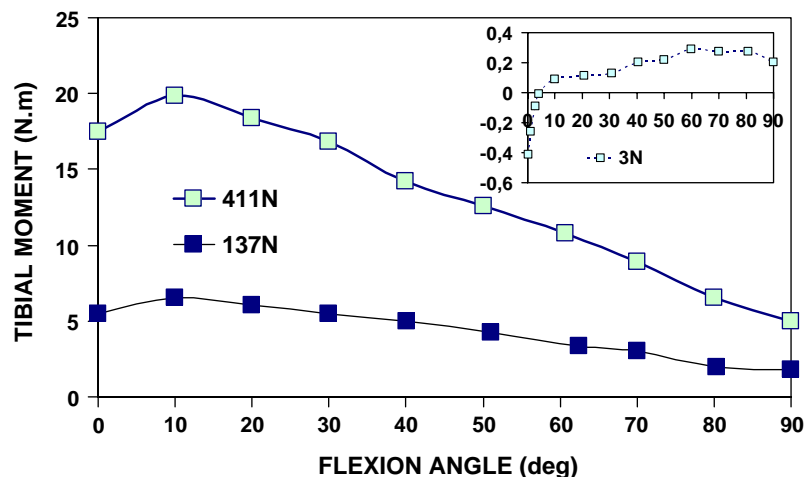


Fig. 10. Extensor joint moment on the tibia under  $F_Q=3$ , 137, and 411 N at different flexion angles.

menisci, articular cartilage layers, major ligaments, patellar tendon, and quadriceps muscle components was developed and used to analyse the detailed elastostatic response of the entire knee joint at different flexion angles. Three different magnitudes of 3 N (i.e., passive joint), 137 N, and 411 N were chosen for quadriceps forces ( $F_Q$ ) that remained constant during the entire joint flexion. These forces were distributed among three primary components of quadriceps muscle group acting at different directions. For stable and unconstrained boundary conditions, the femur was fixed while the patella and tibia were left completely free. To examine the effect of boundary conditions, under  $F_Q = 137$  N, another stable and unconstrained case was considered in which the femur was flexed with free translations while the tibia was left free only in coupled I/E and V/V rotations. Moreover, apart from the reference cases in which the tibial resistance to quadriceps activation was provided via sagittal moments, to compare with measurement studies, cases (at  $0^\circ$  and  $90^\circ$  under 411 quadriceps force) were also investigated in which the tibia was restrained by forces applied at 20 or 30 cm distal to the TF joint level. The results confirmed the importance of quadriceps forces and boundary conditions on kinematics and load distribution of the entire joint during knee flexion.

#### 4.1. Modelling issues

The joint reference configuration for each quadriceps load case was initially established by applying ligament pre-strains and quadriceps forces. The computed translations for each bony structure was given at a primary node and, hence, would alter had another point been selected for this purpose. The location of primary nodes has, however, no influence what-so-ever on other predictions. Due to the occurrence of finite rotations, an adequate joint coordinate system [47] was selected for presentation of tibial and patellar coupled rotations which were defined about convective local coordinate systems. Comparison of results using three levels of mesh refinement demonstrated the relative adequacy of the model used in this study.

In this study, the stable and fully unconstrained boundary conditions of the femur fixed while the tibia and patella completely free were considered as reference conditions. To investigate the effect of changes in boundary conditions on results, another set similar to that used in our passive tibiofemoral studies was also applied with the femur flexing and the tibia free in coupled rotations only [41–43]. Apart from expected changes in kinematics and in components of contact forces, the results on ligament and resultant contact forces/areas remained almost identical suggesting the equivalence of these unconstrained boundary conditions.

Measurement investigations in the literature have often represented the extensor mechanism by a single force through the central quadriceps tendon aligned with the

rectus femoris [14,17,21,24,25,28,29,48,49]. Ahmed et al. [16] and Powers et al. [30] reported that anatomically-based distribution of the quadriceps force among various muscle components rather than the more traditional axial loading at only the RF component markedly influenced the joint kinematics, contact characteristics, and PF joint reaction (PFJR) force. Sakai et al. [7] also demonstrated the importance of proper consideration of the directions/force ratios of quadriceps components. In the current work, the quadriceps force was distributed among three components in different proportions and directions, according to the  $Q$ -angle model [7]. No sensitivity analysis on lines of actions or relative force magnitudes was, however, carried out. Moreover, no tendofemoral articulations between the quadriceps tendon and the femur were simulated at larger flexion angles. Such contacts have, however, been observed at and beyond  $\sim 90^\circ$  joint flexion angles [22].

To investigate the joint response at different flexion angles, measurement studies often choose to restrain the tibial anterior translation in order to counterbalance the extensor moment of quadriceps forces while preserving the joint flexion at a desired level [12–16,30–36]. This constraint, however apart from generating the desired extensor moment, introduces posterior forces on the tibia the magnitude of which depends on the distal location of restraint (i.e., moment arm) as well as the extensor moment (i.e., quadriceps force). Ahmed et al. [16] acknowledged the effect of this restraint lever arm on results and estimated that any moment arm  $> 40$  cm had no discernible effect on the pressure distribution on the retropatellar surface. Others [34,35] studied the effect of changes in the restraint lever arm on ACL force and the A-P shear force at the TF joint. They reported that ACL force and tibial anterior translation significantly increased as the resisting force shifted distally away from the joint (i.e., larger restraint lever arm). Our results fully corroborate these findings. To resist the extensor moment under a constant  $F_Q = 411$  N, posterior forces of 82.5 N at  $0^\circ$  and 23 N at  $90^\circ$  were required at 20 cm away from the TF joint level which decreased to 56.1 and 15.7 N at 30 cm distance. These forces resulted in substantially larger tibial translations which significantly diminished ACL forces at smaller flexion angles and increased PCL forces at larger flexion angles (Fig. 5). These effects were more pronounced at larger extensor moments (associated with smaller joint angles and/or larger quadriceps forces) and under larger restraining forces (associated with closer location to the joint and/or larger quadriceps forces). In our reference cases, the tibial flexion rotations were prescribed resulting in only a pure sagittal moment on the tibia with no artefact A-P shear force. It is to be noted, however, that the presence of these shear forces are essential if isometric extension exercises against a resistance is simulated. Proper consideration of these forces (artefact or not) is absolutely essential in precise assess-



ment of data accuracy and in subsequent comparison of results of various experimental and model investigations.

#### 4.2. Comparisons and implications

While attempting to evaluate and compare results of various studies, due attention should be paid not only to the well-known inter-specimen variations in geometry and material properties but also to the foregoing discussed issues on boundary conditions, additional (artefact or not) forces that vary with location of restraint, coordinate systems, location of measurements (i.e., primary nodes), quadriceps loading magnitudes/configurations, and the reference configuration with respect to which kinematics data are reported. In flexion and under different quadriceps forces, the patella translated laterally/posteriorly/distally, flexed, rotated medially, and tilted laterally. These displacements are in general agreement with measurements [2,4,6,50–52]. Some works have, however, reported medial shift [3,6], medial tilt [53], and lateral rotation [3,6,26,53].

The tibia translated medially/posteriorly/proximally and rotated in varus and internal directions as joint flexed, in agreement with measurements [3]. At full extension, the tibia experienced anterior translation that increased with the quadriceps forces. Quadriceps forces also increased the tibial internal rotation at larger flexion angles. Previous measurements under single quadriceps force action have reported tibial anterior translation and internal rotation that increase up to  $\sim 30^\circ$  joint flexion and decrease thereafter [12,14,54–56]. These observations are due primarily to the orientation of patellar tendon that pulls anteriorly on the tibia at smaller flexion angles [12].

The tibial anterior translation at full extension under quadriceps forces generated a large ACL tensile force, which diminished with flexion. The ACL force increased proportionally with the quadriceps force. In contrast, greater quadriceps forces decreased PCL forces and caused a delay in their mechanical function at larger flexion angles (Fig. 5). The computed influence of quadriceps forces on ACL and PCL forces are in agreement with reported measurements [10–14,35,56–58]. In agreement with our predictions, ACL force has been reported to substantially vary with changes in the restraint level arm [34,35]. The increase in the ACL force due to quadriceps activations, especially at smaller flexion angles, suggests a higher risk for the ACL or its graft. Rehabilitation exercises at near full extension that demand large quadriceps exertions without hamstrings should, hence, be avoided in post ACL reconstruction period, specially when the restraining force is placed far from the joint [34]. As for a PCL graft, quadriceps exertions tend to diminish their axial force but the restraining force, especially when placed closer to the joint, increases PCL forces at larger flexion angles.

The patellar tendon (PT) force was almost equal to the quadriceps force,  $F_Q$ , at full extension but substantially decreased with flexion to reach  $\sim 30\%$  of the applied  $F_Q$ .

This variation confirms that the PF joint does not act as a pulley [17,24,28]. Using a single quadriceps loading vector, the  $PT/F_Q$  ratio has been reported to vary in the range of  $\sim 1.2$  at  $30^\circ$  to  $0.5$  at  $90^\circ$  flexion [17] and of  $1.16$  at  $10^\circ$  to  $0.64$  at  $70^\circ$  [24]. The substantial relative decrease in the patellar tendon force in flexion points to the higher risk of disruption to the repair or avulsion of the tibial tubercle osteotomy (performed for exposure at total knee arthroplasty [59,60]) in post operative rehabilitation activities involving greater quadriceps forces at near full extension positions. It also supports, for the same reasons, exposure attempts performed below the patella rather than above it [60]. The decrease in PT force with flexion was also responsible for the reduction in the joint extensor moment with flexion and that despite the posterior shift in the tibiofemoral contact [61,62] that tends to increase the lever arm of the extensor mechanism. This latter increase was, however, offset by a decrease in the lever arm due to changes in the orientation of PT force at larger flexion angles.

The resultant contact force at PF articulation significantly increased with joint flexion, a prediction in agreement with reported measurements [17,23]. In contrast to PF contact force, resultant TF contact force decreased during flexion, a trend that is consistent with the substantial decrease in the patellar tendon force in flexion. Similar to the computed PT force, the joint extensor moment (i.e., tibial moment) increased with greater  $F_Q$  force but decreased with joint flexion, a variation in good agreement with measurements [31].

The PF contact area increased from  $103 \text{ mm}^2$  at full extension to  $320 \text{ mm}^2$  at  $30^\circ$  and to a maximum of  $356 \text{ mm}^2$  at  $90^\circ$ . Ahmed et al. [17] reported a substantial increase in PF contact area with the joint flexion reaching at  $90^\circ$  values of  $400$  and  $460 \text{ mm}^2$  under quadriceps forces of  $734$  and  $1468 \text{ N}$ , respectively. Under variable quadriceps forces balancing external moments of  $35.1 \text{ N}\cdot\text{m}$  at  $30^\circ$  and  $33.9 \text{ N}\cdot\text{m}$  at  $90^\circ$ , the PF contact area was measured to increase from  $138 \text{ mm}^2$  at  $30^\circ$  to  $328 \text{ mm}^2$  at  $90^\circ$  [63]. At larger flexion angles, disagreement exists as if the PF contact area remains constant [17,64,65], decreases [49,66], or increases [63]. Under compressive load, Ahmed et al. [17] reported that TF contact area decreased with the knee flexion which tends to agree with our predictions.

The ratio of extensor moments calculated at different flexion angles under  $F_Q=411$  and  $137 \text{ N}$  was found to remain constant at  $\sim 3$  as the joint flexed from  $0^\circ$  to  $90^\circ$ . Similarly, an almost linear relation between the  $F_Q$  and extensor moment has been reported [13]. The equivalent lever arm of the extensor mechanism, defined as the ratio of the extensor moment over PT force, remained at different flexion angles nearly the same as the  $F_Q$  increased from  $137$  to  $411 \text{ N}$ . This value, however under  $F_Q=411 \text{ N}$ , initially increased from  $\sim 43 \text{ mm}$  at full extension to  $\sim 49 \text{ mm}$  at  $10^\circ$  flexion and subsequently decreased to  $\sim 41 \text{ mm}$  at  $90^\circ$ .

Finally, the effect of changes in the magnitude of quadriceps forces and in the manner in which the tibia is restrained on joint kinematics and load distribution was computed to be significant throughout flexion. The PT force, ACL force, TF resultant contact force/area and joint extensor moment all increased with greater quadriceps forces but substantially decreased as the joint flexed from full extension to 90° flexion. In contrast, PF resultant contact force/area increased also with the joint flexion to reach its maximum at 90° flexion. Restraining the tibial extensor moment by perpendicular forces tends to substantially decrease ACL forces at smaller flexion angles whereas to significantly increase PCL forces at larger flexion angles. These effects will increase with larger quadriceps forces or less distal placement of restraining forces. Future model studies should delineate the likely interactions between quadriceps/hamstrings muscle exertions and cruciate ligament forces on one hand and their combined effects on articular cartilage contact stresses/areas on the other.

### Acknowledgements

The financial support of the Natural Science and Engineering Research Council of Canada (NSERC-Canada) and FCAR-Québec are gratefully acknowledged. The earlier efforts of M.Z. Benjaballah and K.E. Moglo are also gratefully acknowledged.

### References

- [1] Dehaven KE, Lintner DM. Athletic injuries: comparison by age, sport, and gender. *Am J Sports Med* 1986;14:218–24.
- [2] Hsu HC, Luo ZP, Rand JA, An KN. Influence of patellar thickness on patellar tracking and patellofemoral contact characteristics after total knee arthroplasty. *J Arthrop* 1996;11:69–80.
- [3] Kwak SD, Ahmad CS, Gardner TR, Greslamer RP, Henry JL, Blankevoort L, et al. Hamstrings and iliotibial band forces affect knee kinematics and contact pattern. *J Orthop Res* 2000;18:101–8.
- [4] Nagamine R, Otani T, White SE, McCarthy DS, Whiteside LA. Patellar tracking measurement in the normal knee. *J Orthop Res* 1995;13:115–22.
- [5] Li G, Zayontz S, DeFrate LE, Most E, Suggs JF, Rubash HE. Kinematics of the knee at high flexion angles: an in vitro investigation. *J Orthop Res* 2004;22:90–5.
- [6] Reider R, Marshall JL, Ring B. Patellar tracking. *Clin Orthop* 1981;157:143–8.
- [7] Sakai N, Luo ZP, Rand JA, An KN. Quadriceps forces and patellar motion in the anatomical model of the patellofemoral joint. *The Knee* 1996;3:1–7.
- [8] von Eisenhart-Rothe R, Siebert M, Bringmann C, Vogl T, Englmeier K-H, Graichen HA. New in vivo technique for determination of 3D kinematics and contact areas of the patello-femoral and tibio-femoral joint. *J Biomech* 2004;37:927–34.
- [9] Beynon BD, Fleming BC, Johnson RJ, Nichols CE, Renstrom PA, Pope MH. Anterior cruciate ligament strain behavior during rehabilitation exercises in vivo. *Am J Sports Med* 1995;23:24–34.
- [10] Beynon BD, Fleming BC. Anterior cruciate ligament strain in vivo: a review of previous work. *J Biomech* 1998;31:519–25.
- [11] Draganich LF, Vahey JW. In vitro study of anterior cruciate ligament strain induced by quadriceps and hamstrings forces. *J Orthop Res* 1990;8:57–63.
- [12] Hsieh Y-F, Draganich LF. Increasing quadriceps loads affect the lengths of the ligaments and the kinematics of the knee. *J Biomech Eng* 1998;120:750–6.
- [13] Hsieh Y-F, Draganich L.F. Knee kinematics and ligament lengths during physiologic levels of isometric quadriceps loads. *The Knee* 1997;4:145–54.
- [14] Li G, Rudy TW, Sakane M, Kanamori A, Ma CB, Woo SL-Y. The importance of quadriceps and hamstring muscle loading on knee kinematics and in situ forces in the ACL. *J Biomech* 1999;32:395–400.
- [15] Markolf KL, O'Neill G, Jackson SR, McAllister DR. Effects of applied quadriceps and hamstrings muscle loads on forces in the anterior and posterior cruciate ligaments. *Am J Sports Med* 2004;32(5):1144–9.
- [16] Ahmed AM, Burke DL, Yu A. In vitro measurement of static pressure distribution in synovial joints: Part II. Retropatellar surface. *J Biomech Eng* 1983;105:226–35.
- [17] Ahmed AM, Burke DL, Hyder A. Force analysis of the patellar mechanism. *J Orthop Res* 1987;5:69–85.
- [18] Aeshian GA, Kwak SD, Soslowsky LJ, Mow VC. Stereophotogrammetric method for determining in situ contact areas in diarthrodial joints, and a comparison with other methods. *J Biomech* 1994;27:111–24.
- [19] Brechter JH, Powers CM. Patellofemoral joint stress during stair ascent and descent in persons with and without patellofemoral pain. *Gait Posture* 2002;16:115–23.
- [20] Fukukubayashi T, Kurosawa H. The contact area and pressure distribution pattern of the knee, a study of normal and osteoarthritic knee joints. *Acta Orthop Scand* 1984;51:871–9.
- [21] Huberti HH, Hayes WC, Stone JL, Shybut GT. Force ratios in the quadriceps tendon and ligamentum patellae. *J Orthop Res* 1984;2:49–54.
- [22] Matsuda S, Ishinishi T, White SE, Whiteside LA. Patellofemoral joint after total knee arthroplasty. Effect on contact area and contact stress. *J Arthroplast* 1997;12:790–7.
- [23] Singerman R, Berilla J, Davy DT. Direct in vitro determination of the patellofemoral contact force for normal knees. *J Biomech Eng* 1995;117:8–14.
- [24] Buff H-U, Jones LC, Hungerford DS. Experimental determination of forces transmitted through the patello-femoral joint. *J Biomech* 1988;21:17–23.
- [25] Goodfellow J, Hungerford DS, Zindel M. Patellofemoral joint mechanics and pathology: functional anatomy of the patellofemoral joint. *J Bone Jt Surg* 1976;58-B:287–90.
- [26] Heegaard J, Leyvraz PF, Curnier A, Rakotomanana L, Huiskes R. The biomechanics of the human patella during passive knee flexion. *J Biomech* 1995;28:1265–79.
- [27] Hirokawa S. Three-dimensional mathematical model analysis of the patellofemoral joint. *J Biomech* 1991;24:659–71.
- [28] Huberti HH, Hayes WC. Patellofemoral contact pressures: the influence of Q-angle and tendofemoral contact. *J Bone Jt Surg* 1984;66-A:715–24.
- [29] Huberti HH, Hayes WC. Contact pressures in chondromalacia patellae and the effects of capsular reconstructive procedures. *J Orthop Res* 1988;6:499–508.
- [30] Powers CM, Lilley JC, Lee TQ. The effects of axial and multi-plane loading of the extensor mechanism on the patellofemoral joint. *Clin Biomech* 1998;13:616–24.
- [31] Draganich LF, Andriacchi TP, Andersson GBJ. Interaction between intrinsic knee mechanics and knee extensor mechanism. *J Orthop Res* 1987;5:539–47.
- [32] Farahmand F, Tahmasbi MN, Amis A. Lateral force-displacement behaviour of the human patella and its variation with knee flexion—a biomechanical study in vitro. *J Biomech* 1998;31:1147–52.

- [33] Farahmand F, Tahmasbi MN, Amis A. The contribution of the medial retinaculum and quadriceps muscles to patellar lateral stability—an in vitro study. *The Knee* 2004;11:89–94.
- [34] Jurist KA, Otis JC. Anteroposterior tibiofemoral displacements during isometric extension efforts. The roles of external load and knee flexion angle. *Am J Sports Med* 1985;13:254–8.
- [35] Pandy MG, Shelburne KB. Dependence of cruciate-ligament loading on muscle forces and external load. *J Biomech* 1997;30:1015–24.
- [36] Senavongse W, Farahmand F, Jones J, Andersen H, Bull AMJ, Amis AA. Quantitative measurement of patellofemoral joint stability: force-displacement behavior of the human patella in vitro. *J Orthop Res* 2003;21:780–6.
- [37] Bendjaballah MZ, Shirazi-Adl A, Zukor DJ. Finite element analysis of human knee joint in varus–valgus. *Clin Biomech* 1997;12:139–48.
- [38] Bendjaballah MZ, Shirazi-Adl A, Zukor DJ. Biomechanical response of the passive human knee joint under anterior–posterior forces. *Clin Biomech* 1998;13:625–33.
- [39] Hull ML, Donahue TLH, Rashid MM, Jacobs CR. A finite element model of the human knee joint for the study of tibio–femoral contact. *J Biomech Eng* 2002;124:273–80.
- [40] Li G, Lopez O, Rubash H. Variability of a three-dimensional finite element model constructed using magnetic resonance images of a knee for joint contact stress analysis. *J Biomech Eng* 2001;123:341–6.
- [41] Moglo KE, Shirazi-Adl A. On the coupling between anterior and posterior cruciate ligaments, and knee joint response under anterior femoral drawer in flexion: a finite element study. *Clin Biomech* 2003;18:751–9.
- [42] Moglo KE, Shirazi-Adl A. Biomechanics of passive knee joint in drawer: load transmission in intact and ACL-deficient joints. *The Knee* 2003;10:265–76.
- [43] Moglo KE, Shirazi-Adl A. Cruciate coupling and screw-home mechanism in passive knee joint during extension–flexion. *J Biomech* 2005;38:1075–83.
- [44] Atkinson P, Atkinson T, Huang C, Doane R. A comparison of the mechanical and dimensional properties of the human medial and lateral patellofemoral ligaments. *Transactions of the 46th Annual Meeting of the Orthopaedic Research Society, Orlando*, p. 776.
- [45] Butler DL, Kay MD, Stouffer DC. Comparison of material properties in fascicle-bone units from human patellar tendon and knee ligaments. *J Biomech* 1986;19:425–32.
- [46] Stäubli HU, Schatzmann L, Brunner P, Rincon L, Nolte LP. Mechanical tensile properties of the quadriceps tendon and patellar ligament in young adults. *Am J Sports Med* 1999;27:27–34.
- [47] Grood ES, Suntay WJ. Joint coordinate system for the clinical description of three-dimensional motions: application to the knee. *J Biomech Eng* 1983;105:136–44.
- [48] Lee TQ, Anzel SH, Bennett KA, Pang D, Kim WC. The influence of fixed rotational deformities of the femur on the patellofemoral contact pressures in human cadaver knees. *Clin Orthop Relat Res* 1994;302:69–74.
- [49] Mathews LS, Sonstegard DA, Henke JA. Load bearing characteristics of the patellofemoral joint. *Acta Orthop Scand* 1977;48:511–6.
- [50] Ahmad CS, Kwak SD, Ateshian GA, Warden WH, Steadman JR, Mow VC. Effects of patellar tendon adhesion to the anterior tibia on knee mechanics. *Am J Sports Med* 1998;26:715–24.
- [51] Ahmed AM, Duncan NA, Tanzer M. In vitro measurement of the tracking pattern of the human patella. *J Biomech Eng* 1999; 121:222–228.
- [52] van Kampen A, Huiskes R. The three-dimensional tracking pattern of the human patella. *J Orthop Res* 1990;8:372–82.
- [53] Mizuno Y, Kumagai M, Mattessich SM, Elias JJ, Ramrattan N, Cosgarea AJ, et al. Q-angle influences tibiofemoral and patellofemoral kinematics. *J Orthop Res* 2001;19:834–40.
- [54] Hoher J, Vogrin TM, Woo SL-Y, Carlin GJ, Aroen A, Harner CD. In situ forces in the human posterior cruciate ligament in response to muscle loads: a cadaveric study. *J Orthop Res* 1999;17:763–8.
- [55] Li G, Gill TJ, DeFrate LE, Zayontz S, Glatt V, Zarins B. Biomechanical consequences of PCL deficiency in the knee under simulated muscle loads—an in vitro experimental study. *J Orthop Res* 2002;20:887–92.
- [56] Li G, Zayontz S, Most E, DeFrate LE, Suggs JF, Rubash HE. In situ forces of the anterior and posterior cruciate ligaments in high knee flexion: an in vitro investigation. *J Orthop Res* 2004;22:293–7.
- [57] Li G, Rudy TW, Allen C, Sakane M, Woo SL-Y. Effect of combined axial compressive and anterior tibial loads on in situ forces in the anterior cruciate ligament: a porcine study. *J Orthop Res* 1998;16:122–7.
- [58] Goss BC, Howell SM, Hull ML. Quadriceps load aggravates and roofplasty mitigates active impingement of anterior cruciate ligament grafts against the intercondylar roof. *J Orthop Res* 1998;16:611–7.
- [59] Mendes MW, Caldwell P, Jiranek WA. The results of tibial tubercle osteotomy for revision total knee arthroplasty. *J Arthroplast* 2004; 19(2):167–74.
- [60] Whiteside LA. Exposure in difficult total knee arthroplasty using tibial tubercle osteotomy. *Clin Orthop Relat Res* 1995 (Dec);321:32–5.
- [61] Dennis DA, Mahfouz MR, Komistek RD, Hoff W. In vivo determination of normal and anterior cruciate ligament-deficient knee kinematics. *J Biomech* 2005;38(2):241–53.
- [62] Scarvell JM, Smith PN, Refshauge KM, Galloway H, Woods K. Comparison of kinematics in the healthy and ACL injured knee using MRI. *J Biomech* 2005;38(2):255–62.
- [63] Hsieh YF, Draganich LF, Ho SH, Reider B. The effects of removal and reconstruction of the anterior cruciate ligament on the contact characteristics of the patellofemoral joint. *Am J Sports Med* 2002; 30(1):121–7.
- [64] Hefzy MS, Jackson WT, Saddemi SR, Hsieh YF. Effects of tibial rotations on patellar tracking and patello–femoral contact areas. *J Biomed Eng* 1992;14(4):329–43.
- [65] Hille E, Schultz KP, Henrichs C, Schneider T. Pressure and contact surface measurements within the femoropatellar joint and their variations following lateral release. *Arch Orthop Trauma Surg* 1985;104:1393–401.
- [66] D'Agata SD, Pearsall IV AW, Reider B, Draganich LF. An in vitro analysis of patellofemoral contact areas and pressures following procurement of the central one-third patellar tendon. *Am J Sports Med* 1993;21(2):212–9.